A Theoretical Study on the Electronic Structure of Au−$XO^{(0,-1,+1)}$ (X = C, N, and O) Complexes: Effect of an External Electric Field

Frederik Tielens,*,† Lourdes Gracia, Victor Polo, and Juan Andrés*

Departament de Química Física i Analítica, Universitat Jaume I, Apartat 224, 12080, Castellón, Spain

Received: July 31, 2007; In Final Form: October 1, 2007

A theoretical study on the nature of Au−$XO^{(0,-1,+1)}$ (X = C, N, O) interaction is carried out in order to provide a better understanding on the adsorption process of XO molecules on Au surfaces or Au-supported surfaces. The effect of the total charge as well as the presence of an external electric field on the formation processes of the Au−XO complex are analyzed and discussed using DFT (B3LYP) and high-level *ab initio* (CCSD(T)//MP2) methods employing a 6-311+G(3df) basis set for X and O atoms and Stuttgart pseudopotentials for Au atom. The presence of an electric field can increase the binding of O_2 molecule to Au while weakening the formation of the Au−CO complex. These behaviors are discussed in the context of adsorption or deadsorption of these molecules on Au clusters. The formation of the Au−XO complex, the effect of addition/removal of one electron, and the role of the electric field are rationalized by studying the nature of the bonding interactions by means of the electron localization function (ELF) analysis. The net interaction between Au and XO fragments is governed by the interplay of three factors: (i) the amount of charge transfer from Au to XO, (ii) the sharing of the lone pair from X atom by the Au core (V(X, Au) basin), and (iii) the role of the lone pair of Au (V(Au) basin) mainly formed by 6s electrons. The total charge of the system and the applied electric field determine the population and orientation of the V(Au) basin and, subsequently, the degree of repulsion with the V(X, Au) basin.

1. Introduction

Gold is the most noble of all metals in the periodic table, and due to the known chemical inertness of gold as bulk material, it presents low values of adsorption energies of gases as well as large values of dissociation barriers, which are key factors for most catalytic processes.[1] The detection of gold carbonyls by Mond[2] in 1890 and the oxidation of hydrogen on gold gauze by Bone[3] in 1906 can be considered the first discoveries of catalytic activity of gold. More than a century later, the interest in gold as a catalyst has never been so modern-day; in particular, gold nanoparticles present unique physical and chemical properties being responsible for their remarkable catalytic activity.[4−8] One of the first breakthroughs was the discovery of catalyzed hydrogenation of olefines[9] and low-temperature CO combustion,[10,11] followed by other catalyzed reactions such as propylene epoxidation, NO_x reduction/dissociation, methanol synthesis, SO_2 dissociation, selective oxidation, and water−gas shift (see ref 12 and refs therein). The study of the adsorption of small molecules on gold atoms has been recently summarized in the reviews of Pyykkö,[13,14] while Hashmi[15] has presented a review on gold-catalyzed organic reactions, pointing out the speed at which this research field is expanding nowadays.

Cationic gold carbonyls have been obtained and characterized from the early 1920s.[16] Neutral gold carbonyls[17−21] and gold−carbon systems[22−24] have also been studied, and these compounds are known to have a very weak binding energy (∼0.25 eV). Moreover, they are difficult to detect experimentally and also to calculate theoretically due to their open-shell nature. In spite of these difficulties, the cationic and neutral species have been studied using *ab initio* methods.[19,25] Very recently, their catalytic effect supported on metal oxides has been analyzed,[26−28] as well as the CO adsorption on pure and binary gold clusters.[29]

Despite the importance in recent catalytic discoveries of gold nanoclusters, very few studies have been dedicated to atomic gold mononitrosyls. Ding[30] presented a density functional study on the effect of Au_n ($n = 1-6$) cluster size with different charge states in the adsorption process of NO on Au small clusters. Citra et al.[31] pointed out that laser-ablated gold clusters react with the NO molecule, in excess of argon and neon, yielding the neutral nitrosyl complexes AuNO and $(AuNO)_2$ as the main products. However, there is a lack of both theoretical and experimental studies on anionic Au−NO complexes. From our concern, there is only one theoretical study on the Au−N system.[32]

On the other hand, numerous studies have been published on Au−O_2 systems. The earliest experimental works on these systems were published in the 1970s when McIntoch[33] examined reactions of gold atoms with oxygen, forming the green-colored OAuO molecule. Cox[34] investigated the adsorption of O_2 on gold clusters in the 1990s. Andrews and co-workers,[35,36] via the FTIR matrix technique, observed the neutral Au−O−O molecule in 1999 and characterized it by infrared and ESR spectroscopy, concluding that O_2 binds to gold in a side-on fashion.[35−38] However, in one of these studies, Wang[35] noted some uncertainties on the attachment of O_2 on gold due to the broad isotopic bands observed in the IR spectrum, although DFT calculations supported the formation of the Au−O_2 complex. Whetten's group[39] showed that no exothermic adsorption complex is formed between the neutral Au atom and the O_2

* tielens@ccr.jussieu.fr; andres@qfa.uji.es.

† Present address: Laboratoire de Réactivité de Surface, UMR 7609, Université Pierre et Marie Curie-Paris6, Tour 54-55, 2ème étage - Casier 178, 4, Place Jussieu, F-75252 Paris Cedex 05, France.

10.1021/jp076089d CCC: $37.00
Published on Web 11/17/2007

molecule. Nevertheless, shortly after a thoroughly investigation[40] on the quality of the DFT calculations on the gold oxygen complexes, Sun[37] reconfirmed the existence of AuO_2 theoretically. Moreover, Yoon[41] stated that adsorption will take place on neutral clusters, although weaker than for the anionic one, in line with the odd−even electron number interaction rule discussed by Mills.[42] Concerning the anion, we know from Whetten's postulate that an O_2 molecule can only be adsorbed on Au_n^- anions with an unpaired number of electrons; Au_n^- should not be able to induce a charge transference to form a AuO_2^- complex.[43] Nevertheless, Sun detected AuO_2^- using UPS,[37] and their results about the dissociative adsorption process of O_2 on Au^- are in line with other experimental observations.[44,45] Although Cox[34] did not observe any O_2 adsorption on positively charged Au clusters, the AuO_2^+ complex was detected experimentally during sputtering of a gold target in an $Ar-O_2$ discharge by glow discharge mass spectroscopy,[46] and in our recent pulsed field desorption mass spectroscopy (PFDMS) experiments.[47] Information is lacking on the affinity of atomic and molecular oxygen toward positively charged gold atoms.[40,48,49] To our knowledge, only a few studies deal with this special case; Ding[50] predicted a stable complex on the basis of DFT calculations using hybrid functionals and argued that these complexes were not detected experimentally or they are not competitive compared with the anionic species, due to their low adsorption energy ($E_{bind} < 0.5$ eV). Very recently, theoretical studies predict the adsorption of O_2 on gold nanopyramids[51] and on binary−alloy clusters of gold.[29] Experimentally, it has been shown that O_2 does not adsorb with enough binding energy to be detected on a positively charged tip,[47] in contrast with negatively charged tips.[52]

These studies demonstrate that highly valuable information about the initial steps of Au-catalyzed reactions involving CO, NO, and O_2 molecules can be obtained from experimental and theoretical studies of neutral and charged AuXO (X = C, N, and O) complexes. Two main aspects were found to play a key role in the Au adsorption process: (i) Catalytically active Au particles were suggested to be negatively charged through the charge transfer from defect sites of the oxide support.[53] It was recently shown that Au cluster anions in the gas phase show comparable catalytic activity to those on metal oxide supports, confirming the importance of negative charge on the clusters.[39,43,45] (ii) It is well-known that the presence of an external electric field can cause dramatic changes in reactivity, which can be different from the gas phase. As a result, the complexes become more or less stable dependent on the electric field properties, and can be used as a probe for studying catalytic effects.[47,52]

In order to provide a better understanding on the nature of the interaction between Au and three of the most frequently absorbed molecules (CO, NO, O_2) and to elucidate the role of the total charge, as well as the presence of the electric field, a systematic study based on theoretical calculations is carried out in this work. First, the equilibrium geometry and stabilities of nine Au−XO (X = C, N, O) complexes in neutral and charged forms are calculated at B3LYP and CCSD(T)//MP2 computational levels using the same basis set. Next, the effect of homogeneous electrostatic fields on the complexation energies for the neutral species is investigated. The inclusion of an external electric field is a powerful maneuver to simulate conditions taking place in heterogeneous catalysis involving nanoclusters. Another important issue stands on the nature of the adsorbate−metal bonding, which has been extensively studied for decades[54,55] using models and concepts derived from molecular orbital theory. Recently, previous studies on the Au−O interaction using density-of-state diagrams and Mulliken charges[56] show features from both covalent and ionic bonding types, pointing out the complexity of these systems. The electron localization function (ELF, $\eta(r)$)[57] applied to investigate the nature of chemical bonding[58] has emerged as a useful tool for the understanding of the nature of many different bonding situations, such as metal−ligand complexes for first-row[59,60] and second-row[61,62] metals. Hence, a detailed analysis on the effect of the X atom, the charge, and the electric field on the formation of the Au−XO complexes will be carried out in order to rationalize the trends observed along the previous sections.

2. Theoretical Methods and Computational Details

The calculations were carried out using the standard procedures implemented in *Gaussian03*[63] program (G03). Structural and thermochemical properties associated with the Au−XO interactions are very dependent on the calculation level due to the subtle interplay between orbital and electrostatic interactions. Methods based on density functional theory (DFT) calculations have proven to yield reliable calculations in the case of oxygen−gold interactions.[40] After some preliminary tests on the available functionals within the G03 program, we ended up with the successful B3LYP exchange correlation functional.[64] The choice of the basis set is another important issue for the accurate calculation of Au−CO complexes. Hence, the large 6-311++G-(3df,3pd) basis set[65] was used for C, N, and O atoms, while for Au, the effective core potentials (ECP) of Stuttgart RSC 1993 ECP,[66] taking into account relativistic corrections, was chosen for all calculations carried out (B3LYP, MP2, and CCSD(T)). Other ECP approaches were tested but only the results obtained with the Stuttgart ECP are presented (the results for the other ECP can be found in the Supporting Information). In order to detect possible shortcomings of the B3LYP approach for some complexes, *ab initio* high-level CCSD(T) calculations at MP2 optimized geometries have been carried out to validate the B3LYP results. The basis set superposition error (BSSE) on the DFT complexation energies was calculated using the counterpoise method.[67]

The binding energies are calculated using eq 1, corresponding positive energies to stable bounded systems.

$$D_e = E_{XO} + E_{Au} - E_{AuXO} \quad (1)$$

In order to gain insight into the nature of the electron pairs forming the Au−XO complexes and their variation with X (X = C, N, O), the total charge, or the electric field applied, the calculated structures were analyzed by means of the ELF using the *TopMod* package.[68] An exploration of ELF mathematical properties enables a partition of the molecular position space in basins of attractors, which present a one-to-one correspondence with chemical local objects such as bonds and lone pairs. These basins are either core basins, C(X), or valence basins, V(X, ...), belonging to the outermost shell and characterized by their coordination number with core basins, which is called the synaptic order. From a quantitative point of view, the method allows the integration of the electron density over the basins to provide the basin populations, $\bar{N}$, and integrated spin densities $\langle S_z \rangle$. Moreover, increasing $\eta(\mathbf{r})$ enables the representation of tree diagrams reflecting the hierarchy of the basins.

The effect of an external electric field has been employed to simulate supported gold nanoclusters employed in heterogeneous catalyzed reactions, both experimentally and theoretically.[47,69,70] In order to investigate field effects on the energetics and

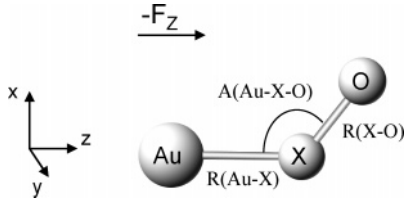

Figure 1. Geometrical parameter definition and orientation of the electric field (−Fz) for Au−XO (X = C, N, and O) complexes.

geometry of XO adsorption, which occur, e.g., on field emitter tips or in general on metal, metal-supported, or metal oxide surfaces, the AuXO complexes are placed in a uniform electrostatic field, F_z (*z*-axis along AuX axis, see Figure 1). Since perpendicular fields and fields along the XO axis yield smaller effects on binding energies and geometry changes, we limit the discussion to the former *z* direction. Using the B3LYP calculation level, an external homogeneous electric field up to 1.25 V/Å was introduced using the keyword Field implemented in the G03 program.

3. Results and Discussion

Although some of the systems studied in this section have been previously analyzed in numerous experimental and theoretical works published in the literature, other systems have attracted less attention. Therefore, we carry out a systematic theoretical investigation on the stability and geometrical parameters for the three complexes, considering neutral, positive, and negative charged species. The performance of B3LYP calculations will be validated against much more expensive CCSD(T) calculations using the same basis set. In the second section, the effect of the electric field on the formation of Au−XO complexes will be analyzed and discussed, pointing out the implications into adsorption processes of heterogeneous catalysis. Finally, the nature of the Au−XO interaction will be studied using the ELF in order to rationalize the factors underlying the interaction between the monomers and their changes upon addition/removal of one electron and the effect of an electric field.

3.1. Binding Energies and Optimized Geometries for Au−XO$^{(0,-1,+1)}$ Complexes. *3.1.1. Au−CO$^{(0,-1,+1)}$.* Our results on the Au−CO complex (see Table 1) show a very good agreement among the values of binding energy calculated by means of the three methods (B3LYP, MP2, and CCSD(T)) and also with previous theoretical and experimental results, predicting the formation of a stable complex with an experimentally measured dissociation energy of 0.25 eV.[14] The best result is found using the B3LYP method, while the other methodologies give a slight overestimation of D_e. Correspondingly, the equilibrium *R*(Au−C) distance is slightly larger for the B3LYP method compared to the MP2 optimized one, 2.083 Å and 1.921 Å, respectively. The calculated angle *A*(Au−C−O) is more sensitive to the method employed, yielding values of 139.2° and 155.4° for the B3LYP and MP2 computing levels, respectively. The anionic Au−CO complex has not been detected experimentally, and only one DFT study[71] has been published on this system. The theoretical calculations predict that it is substantially less stable than the neutral one, with the binding energy reduced to values of 0.10, 0.18, and 0.03 eV for B3LYP, MP2, and CCSD(T) methods, respectively. Large discrepancies are found in the calculated *R*(Au−C) distance; while the B3LYP optimized values are enlarged to 2.971 Å, MP2 gives 2.062 Å. The anionic complex presents very weak long-range dispersion forces which are known to be underestimated by hybrid DFT methods like B3LYP.[72] On the other hand, the removal of one electron from the neutral specie leads to a $(Au-CO)^+$ complex remarkably stronger than the neutral one; the binding energy increases up to 2.08 eV, while the *R*(Au−C) distance becomes 0.1 Å shorter and the angle *A*(Au−C−O) is opened up to 180°, adopting a linear arrangement.

3.1.2. Au−NO$^{(0,-1,+1)}$. The nitrosyl complex presents stronger binding energies than the carbonyl one. Hence, B3LYP results predicts a D_e value of 0.67 eV, while post-Hartree−Fock methods give values of 0.71 and 0.97 eV for MP2 and CCSD(T) results, correspondingly. The distance *R*(Au−N) is similar to that of the carbonyl complex (∼2 Å), but the angle *A*(Au−N−O) is considerably smaller (∼118°). These results are in agreement with the former DFT studies (see Table 2). Upon addition of one electron, B3LYP results show similar changes to those described for the carbonyl complex: lowering of the binding energy, increment of the *R*(Au−N) distance, and small reduction of the *A*(Au−N−O) angle. Conversely, MP2 binding energy is 0.66 eV, and the geometrical parameters are nearly identical to the neutral complex, while CCSD(T) calculations decrease the binding energy to 0.44 eV, pointing toward an overestimation of the complex formation by MP2 methodology. The case of the positively charged complex presents larger difficulties for the MP2 description; while B3LYP gives results consistent with the trend observed in the carbonyl complex, MP2 calculations do not predict a minimum for the $AuNO^+$ configuration, but reorganizes to a $AuON^+$ structure.

3.1.3. Au−O$_2^{(0,-1,+1)}$. The interaction of the peroxo with gold is weaker than the carbonyl and the nitrosyl ones and presents difficulties for its theoretical calculation due to the small energy gap between high- and low-spin states of O_2. Hence, the interaction of the unpaired electron of Au with O_2 can yield a doublet state or a quartet state depending on the coupling between the three unpaired electrons of both monomers. At large *R*(Au−O) distances, the weak through-space exchange coupling interaction between both monomers yields a high-spin state, whereas at short distances, there is some degree of bond formation between both monomers, and the low-spin state is preferred.

Calculations of the doublet state using unrestricted methodology yields values of $\langle S^2 \rangle = 1.48$ and 1.79 at B3LYP and MP2 levels, respectively, very far from the theoretical value of 0.75, and indicating severe mixing of the doublet with higher states. A more adequate treatment of a doublet state can be achieved by using the restricted-open-shell (RO) formalism. Hence, ROB3LYP and ROMP2 calculations have been performed for the $^2A''$ state of the $Au-O_2$ complex. Both ROB3LYP and ROMP2 methods predict short *R*(Au−O) distances (2.137 and 2.063 Å, respectively) but are unstable with respect to dissociation, $D_e = -0.06$ eV, −0.85 eV, and −0.25 eV for B3LYP, MP2, and CCSD(T), respectively. For the quartet state, the complex is dissociated, yielding a very weakly bound complex. The calculation of the negatively charged complex presents divergent results for DFT and *ab initio* methodologies in the calculation of the triplet state. Hence, B3LYP yields the $^3A''$ state with a very large *R*(Au−O) distance of 3.046 Å, while MP2 predict a $^3A'$ state with a shorter *R*(Au−O) distance (2.146 Å) but very small binding energy (0.04 eV). The ground singlet states are $^1A'$ for B3LYP and MP2 methods, but the former gives a very unstable binding energy −0.58 eV, while the latter presents a medium stability (0.26 eV); addition of higher-order correlation effects destabilizes the complex (−0.06 eV).

In contrast to the former two cases (anion and neutral), the cationic complex has been left aside by the literature, concerning

TABLE 1: Binding Energies (D_e in eV, BSSE-corrected in parentheses) and Geometrical Parameters (R: distances in Å; angles in deg) for the Au...CO Complexes Calculated Using B3LYP, MP2, and CCSD(T)//MP2 Methods

						literature		
		B3LYP	MP2	CCSD(T)	exp[a]	B3LYP[b]	MP2[c]	CCSD(T)[d]
(Au...CO)	D_e/BSSE	0.31(0.28)	0.49	0.43	0.25	0.35	0.27	0.49(0.28)
$^2A'$	R(C−O)	1.137	1.145			1.148	1.152	1.141
	R(Au−C)	2.083	1.921			2.081	1.975	2.007
	A(Au−C−O)	139.2	155.4			139.2	152.9	157
$(Au...CO)^-$	D_e/BSSE	0.10(0.09)	0.18	0.03				
$^1A'$	R(C−O)	1.138	1.185					
	R(Au−C)	2.971	2.062					
	A(Au−C−O)	110.5	120.5					
$(Au...CO)^+$	D_e/BSSE	1.92(1.90)	1.82	1.74	2.08 ± 0.15	2.04		1.66
$^1\Sigma^+$	R(C−O)	1.114	1.127			1.127		1.142
	R(Au−C)	1.953	1.906			1.948		1.976
	A(Au−C−O)	180	180			180		180

[a] Ref 14 for Au−CO and ref 67 for Au−CO*. [b] Ref 87. [c] Ref 89. [d] Ref 44 for Au−CO and ref 88 for Au−CO.

TABLE 2: Binding Energies (D_e in eV, BSSE-corrected in parentheses) and Geometrical Parameters (R: distances in Å; angles in deg) for the Au...NO Complexes Calculated Using B3LYP, MP2, and CCSD(T)//MP2 Methods

		B3LYP	MP2	CCSD(T)	exp[a]	lit[b]
(Au...NO)	D_e	0.67(0.65)	0.71	0.97		0.76
$^1A'$	R(N−O)	1.148	1.153			1.15
	R(Au−N)	2.093	2.018			2.08
	A(Au−N−O)	118.3	118.6		140 ± 10	118.4
$(Au...NO)^-$	D_e	0.37(0.36)	0.64	0.44		0.44
$^2A''$	R(N−O)	1.192	1.235			1.20
	R(Au−N)	2.376	2.010			2.32
	A(Au−N−O)	116.9	118.4			116.9
$(Au...NO)^+$	D_e	1.45(1.43)	interaction via oxygen (no minimum for $AuNO^+$)			1.54
$^2A'$	R(N−O)	1.116				1.12
	R(Au−N)	2.161				2.11
	A(Au−N−O)	125.6				125.5

[a] Ref 23. [b] Ref 54.

theoretical calculations, because it is expected that the negative Au_n clusters are more catalytically active. Our calculations predict an exothermic binding energy of 0.49 eV (B3LYP) and 0.30 eV (MP2). The CCSD(T) result is 0.38 eV, which confirms the stability of the complex.

3.2. Effect of Electric Field on Au−XO Complexes. The presence of an electrostatic field improves the charge-transfer process from the XO molecule to the gold atom or vice versa, increasing the binding between both species independent of the field direction, due to orbital reorganizations.[47,52] However, as has been shown in our former works,[47,70] this is not a guarantee that the complex can be detected experimentally.

The effect of the field can be understood by adding a potential energy, $eF_z z$, to the energy of the electrons.[73] This will modify the electronic orbitals and raise the (adjusted) atomic energy levels of Au relative to X and O by approximately $eF_z(z_{Au} - z_X)$ and $eF_z(z_{Au} - z_O)$ and the orbitals of O relative to X by $eF_z(z_O - z_X)$. The alignment of Au−XO in a uniform electrostatic field with the Au−X axis in the field direction results in a more negative charge being transferred into the antibonding $2\pi^*$ molecular orbital of the XO moiety.[47,52] This strengthens the Au−X interaction and, in addition, may establish an electrostatic interaction between the two ends of the complex, due to an increase of its polarization. The Au−XO binding energy increases with the field strength until the limit of one electron is removed from the XO moiety by field ionization. In most cases, the molecules will dissociate into neutral or ionic fragments before the field ionization of the complex is reached.[47] In the case where the field is pointing in the opposite direction, the electronic charge will be taken away from the gold atom, which has the effect of weakening the AuX bond and stabilizing the XO bond. This situation corresponds to the case of a positively charged gold atom, and it is especially interesting for the AuO_2 complex, as will be discussed later on.

TABLE 3: Binding Energies (D_e in eV, BSSE-corrected in parentheses), and Geometrical Parameters (R: distances in Å; angles in deg) for the Au...O_2 Complexes Calculated Using B3LYP, MP2, and CCSD(T)//MP2 Methods

		B3LYP	MP2	CCSD(T)	lit[a]
$(Au...O_2)$	D_e	−0.06(−0.09)	−0.85	−0.23	0.01
$^2A''$	R(O−O)	1.248	1.259		1.22
	R(Au−O)	2.137	2.063		2.30
	A(Au−O−O)	118.2	118.6		118.9
$(Au...O_2)$	D_e	0.00(−0.02)	−0.03	0.06	
$^4A''$	R(O−O)	1.203	1.218		
	R(Au−O)	4.550	3.457		
	A(Au−O−O)	99.8	120.0		
$(Au...O_2)^-$	D_e	0.17(0.16)	0.04	0.08	0.22
$^3A''$ (DFT)	R(O−O)	1.235	1.297		1.24
$^3A'$ (*ab initio*)	R(Au−O)	3.046	2.146		3.05
	A(Au−O−O)	124.2	116.2		124.2
$(Au...O_2)^-$	D_e	−0.58(−0.60)	0.26	−0.06	
$^1A'$	R(O−O)	1.300	1.311		
	R(Au−O)	2.197	2.063		
	A(Au−O−O)	119.0	118.6		
$(Au...O_2)^+$	D_e	0.49(0.47)	0.30	0.38	0.49
$^3A''$	R(O−O)	1.200	1.204		1.20
	R(Au−O)	2.342	2.391		2.28
	A(Au−O−O)	125.2	133.7		122.6

[a] Ref 43.

The geometrical changes of the complex evolve in a similar way (see Table 4). The R(X−O) distance increases while the R(Au−X) distance decreases in negative fields, and in the opposite way for positive electrostatic fields. For strong electric fields, the electronic structure will resemble more and more the

TABLE 4: B3LYP Results of Binding Energies (D_e in eV), Geometrical Parameters (R: distances in Å; angles in deg), Mulliken Atomic Charges (q), and Dipole Moments (μ in debyes), for the Au...XO Complexes Calculated at Different Levels and Methods in an External Electrostatic Field of 1V/Å along the AuX Axis

			D_e	R(X−O)	R(Au−X)	A(Au−X−O)	qX	qO	qAu	μ
Au...CO	^{2}A′	-Fz	0.63	1.166	2.030	133.1	0.185	−0.525	0.341	0.455
	$^2\Sigma^+$	+Fz	0.68	1.117	2.104	180.0	0.410	−0.266	−0.144	
Au...NO	^{1}A′	-Fz	0.94	1.183	2.048	118.8	−0.086	−0.325	0.411	0.400
	^{1}A′	+Fz	1.14	1.110	2.280	119.7	0.570	−0.073	−0.497	
Au...O_2	^{2}A″	-Fz	0.86	1.287	2.158	119.3	−0.212	−0.271	0.482	0.436
	^{2}A″	+Fz	0.20	1.198	2.584	125.4	0.131	0.078	−0.210	

corresponding ion or fragment molecules, and the linear relationship of the distortion disappears, as can be seen in Figures 2 and 3. This effect is particularly notorious for the Au−X distance in AuO_2, where a change in the behavior at higher negative and positive fields can be observed. Another example is the Au−C distance that reaches its minimum quite rapidly for positive fields ($F_z = 0.25$ V/Å). The interaction angle is not affected dramatically in AuO_2 and AuNO complexes. However, the angle of AuCO can have values between 130° and 180°, before ionization or dissociation takes place (see Figure 3).

The NO complex has the highest interaction energy (see Table 4), independent from the applied field. This could be expected, since NO is the molecule having the largest dipole moment and polarizability compared to CO and O_2. On the other hand, CO presents the largest impact of the electric field on its binding energy, which can be associated with the possibility of adapting its geometry to the field. In particular, the flexibility (relatively flat potential energy surface) of the A(Au−C−O) angle (Figure 3) supports this assumption. Concerning the O_2 molecule, an opposite trend is found: there is an increase of the binding energy when a more negative electric field is applied.

In agreement with former results on the Au_{10} cluster,[47,70] a positive electrostatic field increases the binding energy between O_2 and Au; however, they would not be found because of the detection limit (∼0.4 eV) in PFDMS, and the activation energy for ionic dissociation ($Au^+ + O_2$) becomes more favorable with increasing field strength. This result is in line with FEM studies, which have shown that, on a positively charged gold nanotip, CO adsorbs to form mono- and dicarbonyls, although oxygen neither adsorbs nor dissociates. Then, the field direction and their magnitude are important factors in the oxygen adsorption process. It is interesting to point out that for the same field direction there is an opposite effect on the binding energies of CO and O_2 to Au, which can play an important role in possible reactions between both molecules absorbed in the same Au surface. Hence, the (relative) activation of the O_2 molecule only occurs in negative fields, as was shown by McEwen,[52] whereas the opposite effect is found for CO. Although an activation of CO is also seen in negative fields, it is less important than in positive fields.

Besides the effect of the electric field on the Au−XO complexes, it is interesting to consider also the same effect on the two possible fragments separately, namely, Au−X and XO (see Figure 5). Hence, dissociation energies calculated at the same level for CO, NO, and O_2 molecules yield 5.55, 3.37, and 2.96 eV, respectively. The AuX complexes were optimized in their low-spin states, and the results show an increment in the binding energy for more negative electric fields. Interestingly, at fields more negative than −1.25 V/Å (critical field magnitude for dissociative adsorption of O_2), the Au−O bond becomes more stable than the O_2 bond. This result is in agreement with McEwen,[52] who showed that dissociative adsorption only happens for negative fields with a magnitude lower than a critical value (F_c). The Au−C and Au−N binding energies never become higher than the Au−CO (more than 2 eV difference), with the dissociative adsorption being a strongly disfavored process. Moreover, it should be noted that the field is probably enhanced by the cluster size, as the (intrinsic) electric field is as strong on small clusters as it is at the surface of bulk metal.[74]

One can interpret these results in the context of the reactivity of metal oxide supported gold clusters. Since the O_2 and the CO molecules are activated in opposite ways, they will not be adsorbed on the same substrate. This result supports the findings of Vittadini and Selloni,[75] who found in the case of supported Au clusters on TiO_2 that, in contrast to O_2, the CO molecule prefers cationic gold clusters to anionic gold clusters. Another important finding are the DFT calculations of Landman,[76] which revealed that both the presence of F center defect sites and a charge transfer from an oxide support are essential factors in the activation of gold in catalytic systems. Therefore, the fact that the support is implicated, as can be seen from the different experimental results, as well as the importance of the cluster size, supports the suggestion that the oxidation catalysis of CO occurs at the interface between metal and oxide. In other words, the interplay between the right charge transfer of the oxide to CO, and from gold to O_2, is decisive for catalysis of the reaction.

3.3. ELF Analysis of the Nature of Au−XO Interactions: Effect of Electric Field and Charge. Considering the discussion of the previous sections, the strength of the interaction of Au−XO and the equilibrium geometry depends on the nature of the ligand (X = C, N, O), the total charge of the system, and the electric field applied. In order to rationalize these effects, a systematic analysis of the electronic structure using the topology of the ELF is presented here. As was discussed by Silvi,[58] the density arising from the d subshell of Au belongs more to the metal core basin C(Au) than to the valence V(Au). The presence of a V(X, Au) disynaptic basin located near the X atom suggests the classification of the Au−XO interaction as a dative bond. However, contrary to other typical dative bonds characterized by the ELF, the attractor of V(X, Au) is not always located on the line connecting X and Au centers. In some cases, the V(X, Au) basin presents a very low population, and the separation between C(Au) and V(Au) is difficult to characterize in some cases due to the interplay of 5d and 6s electrons on both basins. In Table 5, the topological population analysis data are presented, namely, the basin populations N, integrated spin densities $\langle S_z \rangle$, and net charge transfer (δQ) from the Au atom toward the ligand XO as the difference $\delta Q = \bar{N}[\mathrm{C(Au)}] + \bar{N}[\mathrm{V(Au)}] - Z^{\mathrm{eff}}(\mathrm{Au}) + q$.

In agreement with previous works,[60,62,77] there is a transfer of charge density from the metal to the XO moiety for the neutral compounds. In the case of negatively charged complexes, the amount of δQ is the same as (CO) or larger than (NO, O_2) in the neutral case. For positively charge complexes, the δQ is reduced in comparison to the neutral species, even becoming positive for NO and O_2 systems. Therefore, the analysis of δQ indicates that the addition or removal of one electron takes place

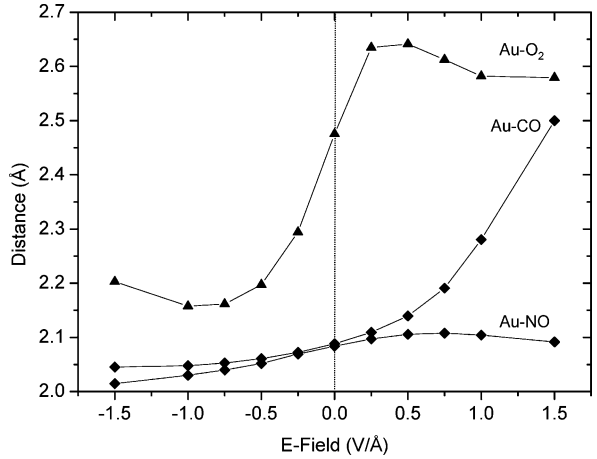

Figure 2. Dependence of the R(Au−X) bond distance in the Au−XO complex with respect to the electrostatic field strength calculated between −1.5 V/Å and 1.5 V/Å.

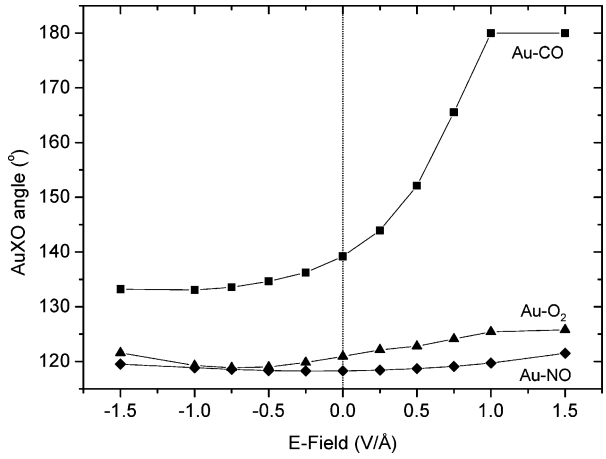

Figure 3. Dependence of the A(Au−X−O) angle in the Au−XO complex versus the electrostatic field strength calculated between −1.5 V/Å and 1.5 V/Å.

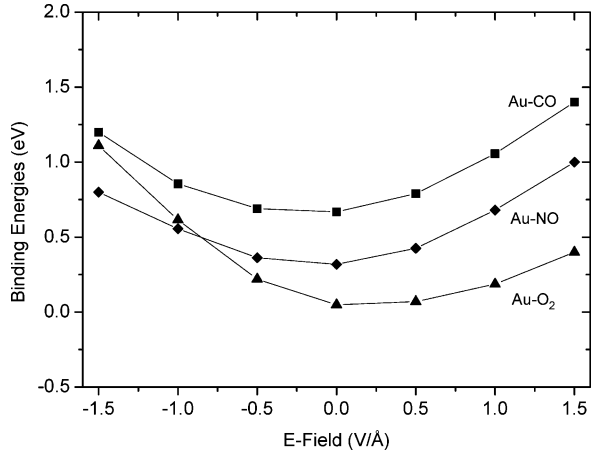

Figure 4. Dependence of the interaction (binding) energies in the Au−XO complex versus the electrostatic field calculated between −1.5 V/Å and 1.5 V/Å.

preferentially on the Au atom. The effect of the electric field also seems to play a role; for CO, there is no noticeable δQ, but for NO and O_2, a negative field moves the electronic charge toward NO and O_2 whereas a positive field acts in the opposite direction.

The populations of the core basin of Au integrates to a much smaller number as expected, due to the use of pseudopotentials,

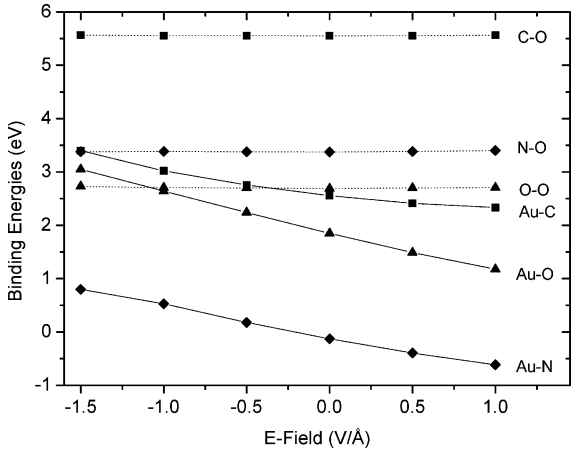

Figure 5. Dependence of the interaction (binding) energies in the Au−X and X−O species versus the electrostatic field calculated between −1.5 V/Å and 1.0 V/Å.

which only consider 18 electrons for core electrons. ELF calculations using an all-electron basis set (WTBS[78,79]) have also been carried out for all CO complexes yielding the correct integration for core electrons while showing only small variations with respect to the basins obtained using the pseudopotential approach (see Supporting Information). Due to the cost of carrying out ELF analysis with such a high number of primitive functions, we continue the study with the Stuttgart ECP results. The C(Au) is not an inert basin, as can be seen from the $\bar{N}$[C(Au)] values of Table 5, and it has to be considered together with the V(Au) basin. Hence, neutral molecules have a C(Au) and V(Au) added population of around 18.70 e, but depending on the X atom and the electric field, a transfer of electronic charge between Au basins can take place. The reduction of localization diagrams displayed in Figure 6 shows the hierarchical order between ELF basins.[80] Hence, two types of diagrams regarding the Au−XO interacting basins are obtained, depending whether the separation between C(Au) and V(Au) occurs for lower (higher) $\eta(r)$ value than the separation between V(X) and C(Au). The populations of basins associated with the XO are consistent with previous ELF investigations. Hence, Lewis mesomeric forms for CO have been studied in detail,[81] and the replacement of C by a more electronegative atom leads to a more covalently depleted bonding type, reducing the $\bar{N}$[V(X, O)] population and increasing $\bar{N}$[V(X)], which can be associated with the presence of more than one lone pair at the X atom.

In all cases, there is a V(X, Au) basin whose population can be very small (0.40 e) or large (3.62 e), and for a comprehensive analysis of these data, they have to be analyzed together with the orientation of the basin and the interaction with the Au atom. A more detailed topological investigation shows that the V(Au) basins can change their number (0, 1, or 2), position, shape, and population depending on the total charge and the field applied, whereas the other basins remain substantially unaltered. In Figure 7, the three-dimensional plot and contour line diagram of the $\eta(r)$ for Au−CO complexes are displayed at the corresponding optimized B3LYP/Stuttgart ECP geometries. For the neutral species, Figure 7a, the V(Au) is located surrounding the Au atom and minimizing the repulsion with the CO basins, integration of the V(Au) electronic charge yields 0.33 e, and it is composed mainly of the 6s orbital. Addition of one electron (Figure 7b) leads to an increment in the volume for the V(Au) basin, and its population rises to 1.89 e. Consequently, the repulsion between the V(Au) and the electron pairs of CO increases, leading to a weakening of the Au−CO interaction.

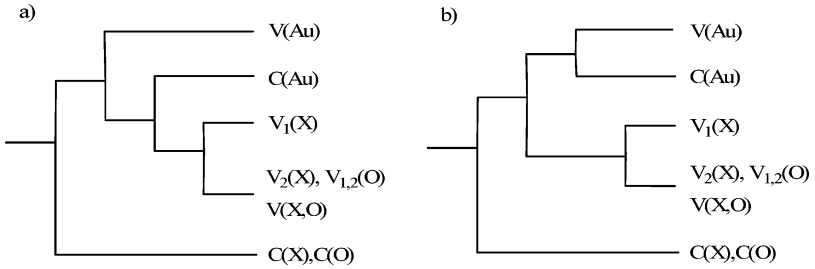

Figure 6. Reduction of localization diagram for AuCO (a) and AuNO, AuO_2 (b).

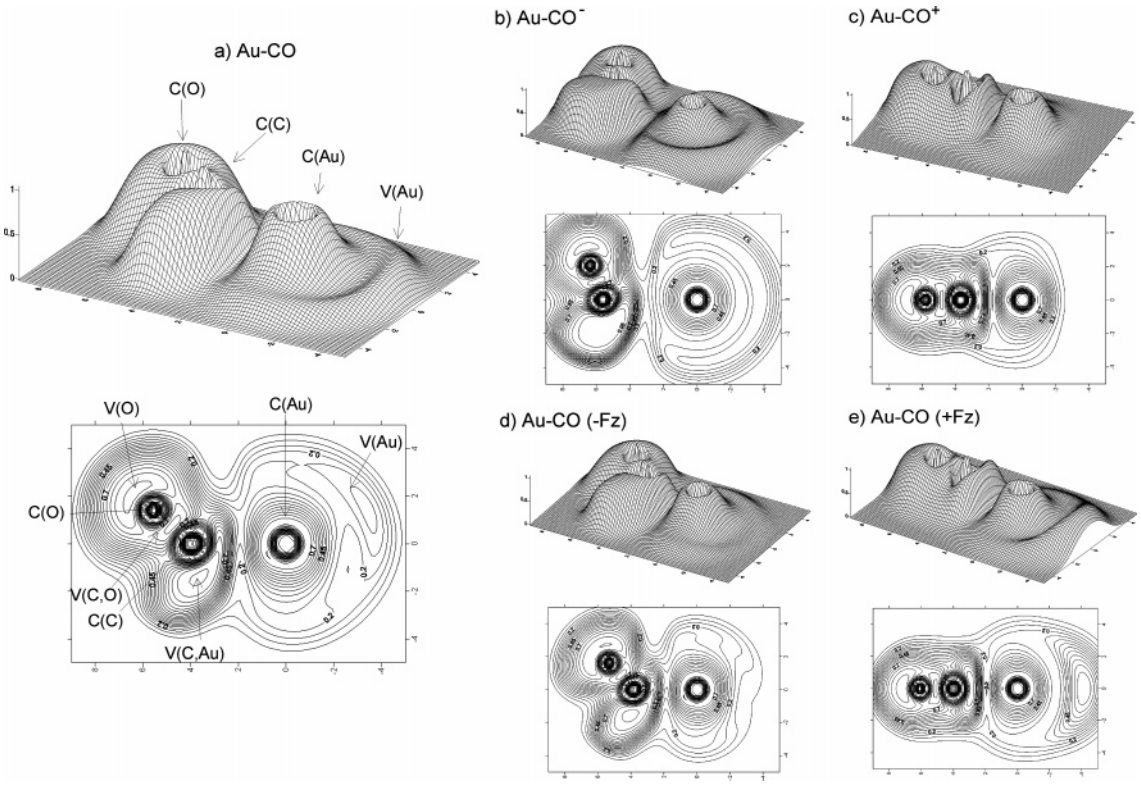

Figure 7. Contour line diagrams and three-dimensional view of the ELF on the plane defined by the atoms for the Au−CO complex (a), negatively (b), and positively charged (c), and with the effect of an electric field in negative (−Fz) (d) and positive (+Fz) (e) orientation.

TABLE 5: ELF Basin Populations $\bar{N}$, Integrated Spin Densities $\langle S_z \rangle$, and Charge Transference (δQ) from Au to XO, Calculated at the Corresponding B3LYP/Stuttgart Optimized Geometry

			C(Au)		V(Au)		V(X,Au)		V(X)		V(X,O)	V(O)		
X	q	field (V/A)	N	$\langle S_z \rangle$	N	$\langle S_z \rangle$	N	$\langle S_z \rangle$	N	$\langle S_z \rangle$	N	N	$\langle S_z \rangle$	δQ
C	0	0	18.40	0.26	0.33	0.10	2.73	0.10	−	−	2.96	4.36	0.02	−0.27
	−1	0	17.84	−	1.89	−	2.65	−	−	−	2.94	4.40	−	−0.27
	1	0	17.86	−	−	−	2.44	−	−	−	2.98	4.54	−	−0.14
	0	−Fz	18.98	0.02	−	−	2.96	0.15	−	−	2.42	4.43	0.03	−0.02
	0	+Fz	18.03	0.17	0.82	0.24	2.54	0.05	−	−	3.33	4.03	−0.01	−0.15
N	0	0	17.65	−	1.21	−	1.17	−	2.67	−	2.20	2.89/2.53	−	−0.14
	−1	0	17.85	−0.01	1.64	−0.02	2.04	0.16	2.12	0.16	1.81	2.86/2.68	0.09	−0.51
	1	0	18.20	0.18	−	−	3.62	0.16	−	0.16	2.46	2.49/2.61	0.07	0.20
	0	−Fz	18.51	−	−	−	1.54	−	2.56	−	1.99	2.94/2.79	−	−0.49
	0	+Fz	17.82	−	1.42	−	3.48	−	−	−	2.49	2.48/2.67	−	0.24
O	0	0	18.19	0.08	0.60	−	0.40	−0.01	4.98	0.18	1.17	2.55/2.35	0.13	−0.21
	−1	0	17.88	0.05	1.75	0.06	2.32	0.18	3.13	0.24	1.08	2.58/2.68	0.20	−0.37
	1	0	18.06	0.05	−	−	2.56	0.18	2.78	0.19	1.27	2.15/2.33	0.25	0.06
	0	−Fz	18.38	−0.06	−	−	1.57	0.04	4.15	0.19	0.93	2.66/2.53	0.15	−0.62
	0	+Fz	18.32	−0.24	0.69	−0.17	2.56	0.19	2.74	0.20	1.28	2.56/1.98	0.24	0.01

On the other hand, removal of one electron leads to the complete disappearance of the V(Au) basin (see Figure 7c), allowing a better interaction between V(C) and C(Au) basins by means of a linear orientation for the maximization of the contact region. The effect of the electric field is also neatly reflected by the polarization of the V(Au) basin (see Figure 7d,e). Hence, the negative field polarizes the V(Au) basin toward the region near the CO, merging the V(Au) basin into the core region as is observed by the increment of $\bar{N}$[C(Au)] to 18.98 e. The change of the orientation of the electric field leads to the opposite behavior, and the V(Au) is now polarized toward the backside, reducing the repulsion with the CO and adopting the same linear

geometry as in the case of the $Au-CO^+$ complex. These behaviors of the V(Au) basin are also observed for the Au−NO and $Au-O_2$ complexes, although the presence of more than one V(X) allows the distribution of the electronic charge between V(X, Au) and V(X) and avoids the linear orientation of the XO for the cases where the repulsion with the V(Au) is very small. These findings are in agreement with recent studies on Pb^{II} compounds where the hemi- or holodirected character of Pb^{II} complexes is explained by the V(Pb) originated by the 6s shell.[82]

4. Conclusions

Using DFT (B3LYP) and *ab initio* (CCSD(T)//MP2) calculations, we have presented a detailed investigation of the equilibrium geometries, electronic structure, and bonding nature of $Au-XO^{(-1,0,+1)}$ (X = C, N, O) complexes and the effect of electric fields. The nature of interaction associated with complex formations is studied by means of the topological analysis of the electron localization function. The main conclusions can be summarized as follows. (i) The stability of Au−XO (X = C, N, O) depends on the three factors considered in this study: the electronegativity of the interacting atom (C, N, O), the total charge of the complex, and the presence of an electric field. (ii) The most stable complexes are $AuCO^+$, AuNO, and AuO_2^+. (iii) For neutral complexes, O_2 adsorption is more stabilized in a negative field environment, while CO adsorption is enhanced in positive fields. (iv) The results are discussed in relation to the reactivity of small gold clusters supported on metal oxides. In this context, it is expected that both the oxygen and CO molecules should not be adsorbed on the same substrate, as they are activated in an opposite way. (v) The interaction between Au and XO is governed by three factors: the amount of charge transferred from Au center to XO fragment, the sharing of lone pair from X atom by the Au core given by the V(X, Au) basin, and the role of the lone pair of Au, V(Au) basin, mainly formed by the 6s electrons. (vi) The effect of the charge and the electric field determines the population and orientation of the V(Au) basin and, subsequently, its degree of repulsion from the V(X, Au) basin.

Acknowledgment. The authors thank Prof. B. Silvi for interesting and stimulating discussions. This work was supported by the Ministerio de Educacion y Ciencia (MEC), DGICYT, CTQ2006-15447-C02-01, Generalitat Valenciana, Projects ACOMP06/122 and GV2007/106, and the Universitat Jaume I-Fundacio Bancaixa, Project P1.1B2004-20. F.T. wishes to thank the Generalitat Valenciana and Fundacio BANCAJA-UJI for financial support to carry out a stay at University Jaume I. L.G. acknowledges the Generalitat Valenciana for providing a Postdoctoral grant (APOSTD07). V.P. thanks support by the Juan de la Cierva fellowship from the MEC. Computer facilities of the Servei d'Informatica (UJI) are also acknowledged.

Supporting Information Available: Benchmark of the ECP on the charged and neutral AuXO complexes (X = C, N, and O). The different Au−XO complexes were calculated using different ECP approaches at the B3LYP and MP2 level. Namely, the Los Alamos LanL2DZ[83−85] double split basis set and the Stevens/Basch/Krauss ECP double split valence basis set (CEP-31)[86−88] were tested, but only the results obtained with the Stuttgart RSC 1997 ECP[66] were retained. This material is available free of charge via the Internet at http://pubs.acs.org.

References and Notes

(1) Hammer, B.; Nørskov, J. K. *Nature (London)* **1995**, *376*, 238.
(2) Mond, L.; Langer, C.; Quincke, F. *J. Chem. Soc.* **1890**, *57*, 749.
(3) Bone, W. A.; Wheeler, R. V. *Philos. Trans.* **1906**, *206A*, 1.
(4) Tielens, F.; Andrés, J. *J. Phys. Chem. C* **2007**, *111*, 10342.
(5) Kita, H.; Nakajima, H.; Hayashi, K. *J. Electroanal. Chem.* **1985**, *190*, 141.
(6) Haruta, M. *Catal. Today* **1997**, *36*, 153.
(7) Valden, M.; Lai, X.; Goodman, D. W. *Science* **1998**, *281*, 1647.
(8) Haruta, M.; Tsubota, S.; Kobayashi, T.; Kageyama, H.; Genet, M. J.; Delmon, B. *J. Catal.* **1993**, *144*, 175.
(9) Bond, G. C.; Sermon, P. A.; Webb, G.; Buchanan, D. A.; Wells, P. B. *J. Chem. Soc.: Chem. Commun.* **1973**, 444.
(10) Hutchings, G. J. *Catal. Today* **2005**, *100*, 55.
(11) Haruta, M. *Nature* **2005**, *437*, 1089.
(12) Stephen, A.; Hashmi, K.; Hutchings, G. J. *Angew. Chem.* **2006**, *45*, 7896.
(13) Pyykkö, P. *Inorg. Chem. Acta* **2005**, *358*, 4113.
(14) Pyykkö, P. *Angew. Chem., Int. Ed.* **2004**, *43*, 4412.
(15) Stephen, A.; Hashmi, K. *Chem. Rev.* **2007**, ASAP.
(16) Manchot, W.; Gall, H. *Chem. Ber.* **1925**, *58*, 2175.
(17) Lupinetti, A. J.; Jonas, V.; Thiel, W.; Strauss, S. H.; Frenking, G. *Chem.—Eur. J.* **1999**, *5*, 2573.
(18) Dargel, T. K.; Hertwig, R. H.; Koch, W. *J. Chem. Phys.* **1998**, *108*, 3876.
(19) Schwerdtfeger, P.; Bowmaker, G. *J. Chem. Phys.* **1994**, *100*, 4487.
(20) Drapprich, S.; Frenking, G. *J. Phys. Chem.* **1995**, *99*, 9352.
(21) Liang, B.; Andrews, L. *J. Phys. Chem. A* **2000**, *104*, 9156.
(22) Pyykkö, P.; Tamm, T. *Theor. Chem. Acc.* **1998**, *99*, 113.
(23) Barysz, M.; Pyykkö, P. *Chem. Phys. Lett.* **2003**, *368*, 538.
(24) Zhai, H. J.; Wang, L. S. *J. Chem. Phys.* **2005**, *122*, 051101.
(25) Mendizabal, F. *Organometallics* **2001**, *20*, 261.
(26) Giordano, L.; Carrasco, J.; Di, Valentin, C.; Illas, F.; Pacchioni, G. *J. Chem. Phys.* **2006**, *125*, 174709.
(27) Klimev, H.; Fajerweg, K.; Chakarova, K.; Dellanoy, L.; Louis, C.; Hadjiivanov, K. *J. Mater. Sci.* **2007**, *42*, 3306.
(28) Arenz, M.; Landman, U.; Heiz, U. *ChemPhysChem* **2006**, *7*, 1871.
(29) Joshi, A. M.; Delgass, W. N.; Thomson, K. T. *J. Phys. Chem. B* **2006**, *110*, 23373.
(30) Ding, X.; Li, Z.; Yang, J.; Hou, J. G.; Zhu, Q. *J. Chem. Phys.* **2004**, *121*, 2558.
(31) Citra, A.; Wang, X.; Andrews, L. *J. Phys. Chem. A* **2002**, *106*, 3287.
(32) Fielicke, A.; von Helden, G.; Meijer, G.; Simard, B.; Rayner, D. M. *Phys. Chem. Chem. Phys.* **2005**, *7*, 3906.
(33) McIntoch, D.; Ozin, G. A. *Inorg. Chem.* **1977**, *16*, 51.
(34) Cox, D. M.; Brinckman, R. O.; Creegan, K.; Kaldor, A. *Mater. Res. Soc. Symp. Proc.* **1991**, *206*, 43.
(35) Wang, X.; Andrews, L. *J. Phys. Chem. A* **2001**, *105*, 5812.
(36) Citra, A.; Andrews, L. *J. Mol. Struct. (THEOCHEM)* **1999**, *489*, 95.
(37) Sun, Q.; Jena, P.; Kim, Y. D.; Fischer, M.; Ganteför, G. *J. Chem. Phys.* **2004**, *120*, 6510.
(38) Kasai, P. H.; Jones, P. M. *J. Phys. Chem.* **1986**, *90*, 4239.
(39) Salisbury, B. E.; Wallace, W. T.; Whetten, R. T. *Chem. Phys.* **2000**, *262*, 131.
(40) Varganov, S. E.; Olson, R. M.; Gordon, M. S.; Metiu, H. *J. Chem. Phys.* **2003**, *119*, 2531.
(41) Yoon, B.; Häkkinen, H.; Landman, U. *J. Phys. Chem. A* **2003**, *107*, 4066.
(42) Mills, G.; Gordon, M. S.; Metiu, H. *J. Chem. Phys.* **2003**, *118*, 4198.
(43) Wallace, W. T.; Whetten, R. T. *J. Am. Chem. Soc.* **2002**, *124*, 7499.
(44) Kim, Y. D.; Fischer, M.; Ganteför, G. *Chem. Phys. Lett.* **2003**, *377*, 170.
(45) Stolcic, D.; Fischer, M.; Ganteför, G.; Kim, Y. D.; Sun, Q.; Jena, P. *J. Am. Chem. Soc.* **2003**, *125*, 2848.
(46) Aita, C. R. *J. Appl. Phys.* **1987**, *61*, 5182.
(47) Visart, de Bocarmé, T.; Chau, T.-D.; Tielens, F.; Andrés, J.; Gaspard, P.; Wang, R. L. C.; Kreuzer, H. J.; Kruse, N. *J. Chem. Phys.* **2006**, *125*, 1.
(48) Liu, W.-J.; van Wüllen, C. *J. Chem. Phys.* **1999**, *110*, 3730.
(49) Mills, G.; Gordon, M. S.; Metiu, H. *Chem. Phys. Lett.* **2002**, *359*, 493.
(50) Ding, X.; Li, Z.; Yang, J.; Hou, J. G.; Zhu, Q. *J. Chem. Phys.* **2004**, *120*, 9594.
(51) Tielens, F.; Andrés, J.; Van, Brussel, M.; Buess-Herman, C.; Geerlings, P. *J. Phys. Chem. B* **2005**, *109*, 7624.
(52) McEwen, J.-S.; Gaspard, P. *J. Chem. Phys.* **2006**, *125*, 214707.
(53) Sanchez, A.; Abbet, S.; Heiz, U.; Schneider, W. D.; Häkkininen, H.; Barnett, R. N.; Landman, U. *J. Phys. Chem. A* **1999**, *103*, 9573.
(54) Newns, D. M. *Phys. Rev.* **1969**, *178*, 1123.
(55) Hammer, B.; Nørskov, J. K. *Adv. Catal.* **2000**, *45*, 71.

(56) Liu, Z. P.; Hu, P.; Alavi, A. *J. Am. Chem. Soc.* **2002**, *124*, 14770.
(57) Becke, A. D.; Edecombe, K. E. *J. Chem. Phys.* **1990**, *92*, 5397.
(58) Silvi, B.; Savin, A. *Nature (London)* **1994**, *371*, 683.
(59) Dobado, J. A.; Molina, J. M.; Uggla, R.; Sundberg, M. R. *Inorg. Chem.* **2000**, *39*, 2831.
(60) Pilme, J.; Silvi, B.; Alikhani, M. E. *J. Phys. Chem. A* **2003**, *107*, 4506.
(61) Michelini, M. D.; Russo, N.; Alikhani, M. E.; Silvi, B. *J. Comput. Chem.* **2005**, *26*, 1284.
(62) Pilme, J.; Silvi, B.; Alikhani, M. E. *J. Phys. Chem. A* **2005**, *109*, 10028.
(63) Frisch, M. J.; Trucks, G. W.; Schlegel, H. B.; Scuseria, G. E.; Robb, M. A.; Cheeseman, J. R.; Montgomery, J., J. A.; Vreven, T.; Kudin, K. N.; Burant, J. C.; Millam, J. M.; Iyengar, S. S.; Tomasi, J.; Barone, V.; Mennucci, B.; Cossi, M.; Scalmani, G.; Rega, N.; Petersson, G. A.; Nakatsuji, H.; Hada, M.; Ehara, M.; Toyota, K.; Fukuda, R.; Hasegawa, J.; Ishida, M.; Nakajima, T.; Honda, Y.; Kitao, O.; Nakai, H.; Klene, M.; Li, X.; Knox, J. E.; Hratchian, H. P.; Cross, J. B.; Bakken, V.; Adamo, C.; Jaramillo, J.; Gomperts, R.; Stratmann, R. E.; Yazyev, O.; Austin, A. J.; Cammi, R.; Pomelli, C.; Ochterski, J. W.; Ayala, P. Y.; Morokuma, K.; Voth, G. A.; Salvador, P.; Dannenberg, J. J.; Zakrzewski, V. G.; Dapprich, S.; Daniels, A. D.; Strain, M. C.; Farkas, O.; Malick, D. K.; Rabuck, A. D.; Raghavachari, K.; Foresman, J. B.; Ortiz, J. V.; Cui, Q.; Baboul, A. G.; Clifford, S.; Cioslowski, J.; Stefanov, B. B.; Liu, G.; Liashenko, A.; Piskorz, P.; Komaromi, I.; Martin, R. L.; Fox, D. J.; Keith, T.; Al-Laham, M. A.; Peng, C. Y.; Nanayakkara, A.; Challacombe, M.; Gill, P. M. W.; Johnson, B.; Chen, W.; Wong, M. W.; Gonzalez, C.; and Pople, J. A. *Gaussian 03*, revision C.02; Gaussian, Inc.: Wallingford, CT, 2004.
(64) Becke, A. D. *J. Chem. Phys.* **1993**, *98*, 5648.
(65) Hehre, W. J.; Radom, L.; Schleyer, P. v. R.; Pople, J. A. *Ab Initio Molecular Orbital Theory*; Wiley: New York, 1986.
(66) Dolg, M.; Stoll, H.; Preuss, H.; Pitzer, R. M. *J. Phys. Chem.* **1993**, *97*, 5852.
(67) Boys, S. F.; Bernardi, F. *Mol. Phys.* **1970**, *10*, 553.
(68) Noury, S.; Krokidis, X.; Fuster, F.; Silvi, B. *Comput. Chem.* **1999**, *23*, 597.
(69) Chai, T.-D.; Visart, de Bocarmé, T.; Kruse, N.; Wang, R. L. C.; Kreuzer, J. *J. Chem. Phys.* **2003**, *119*, 12605.
(70) Tielens, F.; Andrés, J.; Chau, T.-D.; Visart, de Bocarmé, T.; Kruse, N.; Geerlings, P. *Chem. Phys. Lett.* **2006**, *421*, 433.
(71) Wu, X.; Senapati, L.; Nayal, S. K.; Selloni, K.; Hajaligol, M. *J. Chem. Phys.* **2002**, *117*, 4010.
(72) Schwabe, T.; Grimme, S. *Phys. Chem. Chem. Phys.* **2007**, *26*, 3397.
(73) Kreuzer, H. J. *Surf. Interface Anal.* **2004**, *36*, 372.
(74) Suchorski, Y.; Schmidt, W. A.; Ernst, N.; Block, J. H.; Kreuzer, H. J. *Prog. Surf. Sci.* **1995**, *48*, 121.
(75) Vittadini, A.; Selloni, A. *J. Chem. Phys.* **2002**, *117*, 353.
(76) Sanchez, A.; Abbet, S.; Heiz, U.; Schneider, W.-D.; Häkkinen, H.; Barnett, R. N.; Landman, U. *J. Phys. Chem. A* **1999**, *103*, 9573.
(77) Gillespie, R. J.; Noury, S.; Pilme, J.; Silvi, B. *Inorg. Chem.* **2004**, *43*, 3248.
(78) Huzinaga, S.; Miguel, B. *Chem. Phys. Lett.* **1990**, *175*, 289.
(79) Huzinaga, S.; Klobukowski, M. *Chem. Phys. Lett.* **1993**, *212*, 260.
(80) Calatayud, M.; Andrés, J.; Beltrán, A.; V. S. *Theor. Chem. Acc.* **2001**, *105*, 299.
(81) Lepetit, C.; Silvi, B.; Chauvin, R. *J. Phys. Chem. A* **2004**, *107*, 464.
(82) Gourlaouen, C.; Parisel, O. *Angew. Chem., Int. Ed.* **2007**, *46*, 553.
(83) Hay, P. J.; Wadt, W. R. *J. Chem. Phys.* **1985**, *82*, 299.
(84) Hay, P. J.; Wadt, W. R. *J. Chem. Phys.* **1985**, *82*, 270.
(85) Wadt, W. R.; Hay, P. J. *J. Chem. Phys.* **1985**, *82*, 284.
(86) Stevens, W.; Basch, H.; Krauss, J. *J. Chem. Phys.* **1984**, *81*, 6026.
(87) Stevens, W. J.; Krauss, M.; Basch, H.; Jasien, P. G. *Can. J. Chem.* **1992**, *70*, 612.
(88) Cundari, T. R.; Stevens, W. J. *J. Chem. Phys.* **1993**, *98*, 5555.
(89) Hagen, J.; Socaciu, J. D.; Elijazyfer, M.; Heiz, U.; Bernhardt, T. M.; Wöste, L. *Phys. Chem. Chem. Phys.* **2002**, *4*, 1707.